CHEMISTRY OF MATERIALS
Article

Chem. Mater. **2010,** *22,* 5179–5183 5179
DOI:10.1021/cm101085p

Stable Charge-Transfer Doping of Transparent Single-Walled Carbon Nanotube Films

Bhupesh Chandra,[†] Ali Afzali,[†] Neeraj Khare,[‡] Mostafa M. El-Ashry,[§] and George S. Tulevski*[,†]

[†]*IBM T.J. Watson Research Center, Yorktown Heights, New York 10598,* [‡]*Indian Institute of Technology Delhi, Hauz Khas, New Delhi 110 016, India, and* [§]*Egypt Nanotechnology Research Center, Smart Village, Giza 12577, Egypt*

Received April 19, 2010. Revised Manuscript Received June 29, 2010

Single walled carbon nanotube (SWCNT) films are candidates for use as transparent electrodes, especially where low-cost, flexible materials are desired. Chemical doping is a critical step in fabricating conductive films as doping substantially decreases the sheet resistance within SWCNTs and at tube−tube junctions. Despite the importance of chemical doping, surprisingly little effort is devoted to developing doping chemistry. Concentrated acid solutions are typically used to dope SWCNT films. Although they are effective at reducing the sheet resistance of SWCNT films, this method is plagued by two critical drawbacks. The first is that concentrated acid baths, such as HNO_3, are extremely harsh and will damage virtually any device technology. Second, the film resistance is unstable and rises dramatically over time. These drawbacks make implementation of SWCNT transparent, conducting films in technological applications extremely difficult. Here, we report an alternative doping scheme that utilizes a single-electron oxidant (triethyloxonium hexachloroantimonate) to effectively dope the SWCNT films. As evidenced by optical and electrical measurements, the compound effectively p-dopes SWCNT films. In addition to the effective doping, the resultant film resistance is stable over time. The films doped with triethyloxonium hexachloroantimonate outperform nitric acid doped films by a factor of 2.5 over time. This study introduces a new category of chemical dopants that yield stable, transparent, and conductive SWCNT films suitable for technological applications.

Introduction

Transparent conducting electrodes (TCEs) are key components of many modern electronic devices including photovoltaic cells,[1] organic light-emitting diodes,[2] flat panel displays, and touch screens.[3] The most widely used TCE material is indium tin oxide (ITO). Despite the exceptional optoelectronic properties of ITO (sheet resistance of $5 - 10\ \Omega/\square$ at $>85\%$ transmittance), the material suffers from considerable drawbacks including increased materials cost due to the scarcity of indium[4] and the costs associated with high-temperature vacuum deposition.[5] Additionally, vacuum deposited ITO films are brittle and therefore nonideal for use in flexible electronics.[6,7] These significant limitations have motivated the search for alternative materials with single-walled carbon nanotube (SWCNT) films among the leading candidates.[8−16] The advantages of employing SWCNT films as TCEs are that (a) they are synthesized from inexpensive starting materials, (b) produce flexible films, (c) are preferentially hole conductors,[17] and (d) can be processed in solution at room temperature.

The sheet resistance in a network of SWCNTs is limited by the resistance within the SWCNTs and by the junction resistance at tube−tube junctions, the latter being the major contributor.[18−21] Chemical doping is an essential step in lowering both contributions to the sheet resistances.

---

*Corresponding author: E-mail: gstulevs@us.ibm.com.
(1) Pasquier, A. D.; Unalan, H. E.; Kanwal, A.; Miller, S.; Chhowalla, M. *Appl. Phys. Lett.* **2005**, *87*, 203511.
(2) Zhang, D.; Ryu, K.; Liu, X.; Polikarpov, E.; Ly, J.; Tompson, M. E.; Zhou, C. *Nano Lett.* **2006**, *6*, 1880.
(3) Gordon, R. G. *MRS Bull.* **2000**, *25*, 52.
(4) Nature **2007**, *449*, 131.
(5) III-Vs Rev. **2005**, *18*, 12.
(6) Chen, Z.; Cotterell, B.; Wang, W.; Guenther, E.; Chua, S. J. *Thin Solid Films* **2001**, *394*, 202.
(7) Leterrier, Y.; Médico, L.; Demarco, F.; Månson, J.-A. E.; Betz, U.; Escolà, M. F.; Kharrazi, M.; Atamny, F. *Thin Solid Films* **2004**, *460*, 156.
(8) Barnes, T. M.; van de Lagemaat, J.; Levi, D.; Rumbles, G.; Coutts, T. J.; Weeks, C. L.; Britz, D. A.; Levitsky, I.; Peltola, J.; Glatkowski, P. *Phys. Rev. B* **2007**, *75*, 235410.
(9) Gruner, G. *J. Mater. Chem.* **2006**, *16*, 3533.
(10) Hellstrom, S. L.; Lee, H. W.; Bao, Z. *ACS Nano* **2009**, *3*, 1423.
(11) Hu, L.; Hecht, D. S.; Gruner, G. *Nano Lett.* **2004**, *4*, 2513.
(12) Kaempgen, M.; Duesberg, G. S.; Roth, S. *Appl. Surf. Sci.* **2005**, *252*, 425.
(13) Wu, Z.; Chen, Z.; Du, X.; Logan, J. M.; Sippel, J.; Nikolou, M.; Kamaras, K.; Reynolds, J. R.; Tanner, D. B.; Hebard, A. F.; Rinzler, A. G. *Science* **2004**, *305*, 1273.
(14) Yim, J. H.; Kim, Y. S.; Koh, K. H.; Lee, S. *J. Vac. Sci. Technol., B* **2008**, *26*, 851.
(15) De, S.; Lyons, P. E.; Sorel, S.; Doherty, E. M.; King, P. J.; Blau, W. J.; Nirmalraj, P. N.; Boland, J. J.; Scardaci, V.; Joimel, J.; Coleman, J. N. *ACS Nano* **2009**, *3*, 714.
(16) Green, A. A.; Hersam, M. C. *Nano Lett.* **2008**, *8*, 1417.
(17) Lee, K.; Wu, Z.; Chen, Z.; Ren, F.; Pearton, S. J.; Rinzler, A. G. *Nano Lett.* **2004**, *4*, 911.
(18) Barnes, T. M.; Blackburn, J. L.; van de Lagemaat, J.; Coutts, T. J.; Heben, M. J. *ACS Nano* **2008**, *2*, 1968.
(19) Blackburn, J. L.; Barnes, T. M.; Beard, M. C.; Kim, Y.-H.; Tenent, R. C.; McDonald, T. J.; To, B.; Coutts, T. J.; Heben, M. J. *ACS Nano* **2008**, *2*, 1266.

Chemical doping increases the carrier concentration in semiconducting SWCNTs, which make up two-thirds of the SWCNT films. Recent studies show that doping also decreases the tunneling barrier between SWCNTs and conclude that this is the major factor in the overall film resistance.[18,19,21] Concentrated acids, most commonly nitric acid (HNO_3), are typically used to chemically dope the SWCNT films.[18,22−25] The volatility of the acids leads to film resistances that are unstable over time and increases to values approaching those of undoped films.[18,26] In addition, exposing devices to concentrated acid solutions will likely lead to severe degradation of the devices. Despite the importance of chemical doping and the major drawbacks of using concentrated acids, surprisingly little work is published in exploring alternative doping methods.

Herein, we report the use of a single electron oxidant (triethyloxonium hexachloroantimonate, **OA**) to chemically p-dope single-walled carbon nanotube films. The compound forms a charge-transfer complex with the SWCNTs, injecting holes into the SWCNT film. Optical absorption data reveal that the films are highly p-doped and that the doping is stable over time. The electrical measurements support these findings and show that the **OA** doped films outperform acid doped films by a factor of 2.5 over the course of the time study. The charge-transfer complex is stable and nonvolatile, making this method more suitable for technological applications.

Experimental Section

Nanotube Purification through Step-Gradient Centrifugation. SWCNTs are purified via a simple step-gradient centrifugation step (adapted from a previous report)[27] that yields a highly purified, concentrated solution of SWCNTs. Arc-discharge produced SWCNTs are purchased from Iijin Nanotech (www.iljinnanotech.co.kr). The SWCNT powder is mixed with a stock solution of 1% w/v of sodium dodecylsulfate (SDS). The mixture is first sonicated for 5 min with a high power horn sonicator (power, 600W; amplitude, 20%; frequency, 20 kHz), followed by sonication for 30 min in a bath sonicator (1510 Branson). The solution is then centrifuged at 10,000 rpm for 1 h (Beckman Coulter, Optima L-100 XP ultra centrifuge). After centrifugation, the supernatant is collected and then used to fill a centrifuge tube halfway. A 30% Iodixinol (Sigma Aldrich) solution is then layered below the SWCNT/SDS solution to be used as a stop layer. A second centrifugation step is then performed at 41,000 rpm for 18 h. The stop layer produces a narrow band of purified SWCNTs near the middle of the tube, which is collected with a glass pipet. The highly concentrated, purified SWCNT solution is then diluted (1:100 by volume) with the 1% w/v SDS solution. The diluted solution is then briefly sonicated for 10 min in the bath sonicator.

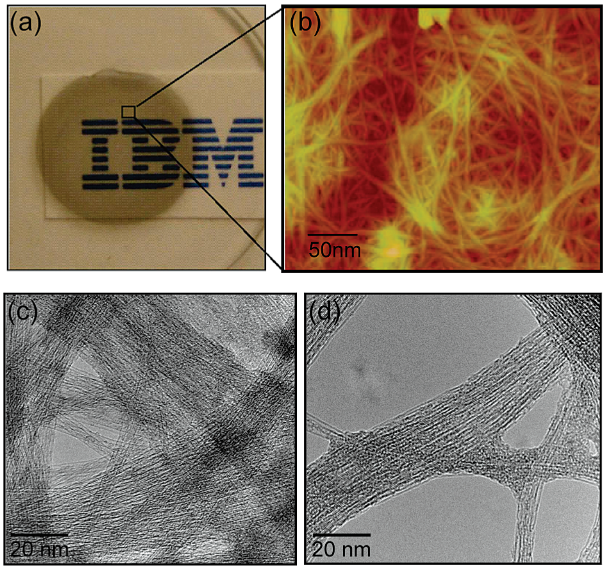

Figure 1. (a) Optical microscope image of a SWCNT film on a quartz substrate. (b) Atomic force microscope (AFM) image of single-walled carbon nanotube film revealing an interlocking network of SWCNT bundles. (c) Transmission electron microscope (TEM) image of an as-prepared, purified SWCNT film. (d) TEM image of a film doped with **OA**. The compound accumulates on the side walls and at tube−tube junctions..

SWNT Film Formation. SWCNT films are fabricated via the vacuum filtration technique.[13] The purified, diluted SWCNT solution is filtered through a mixed cellulose ester membrane (MF-Millipore Membrane, mixed cellulose esters, Hydrophilic, 0.1 μm, 25 mm) to form a uniform SWCNT film. The volume of the SWCNT solution determines the thickness of the SWCNT film. The filtration speed is kept as low as possible to achieve films with a high degree of uniformity. The SWCNT films are then allowed to set for 15−20 min, followed by passing 50 mL of water through the membrane to wash off the residual surfactant. The film is then left to dry in air for 15 min.

The glass substrate is wetted with water to aid in transfer. The membrane, SWCNT-side down, is then pressed onto the wet glass slide. The membrane is then slowly dissolved in acetone, leaving the nanotube film on the glass slide. The SWCNT film is soaked in acetone for 30 min to completely remove the membrane residue.

Chemical Treatments. In order to achieve a high doping efficiency and stability, complete removal of the surfactant is necessary. This is accomplished by exposing the films to 12 M nitric acid for 1 h, followed by rinsing with copious amounts of water. Transmission electron microscopy (TEM) images of the SWCNT films before and after acid cleaning are included in Supporting Information.

The chemical dopant, triethyloxonium hexachloroantimonate (**OA**), was purchased from Sigma Aldrich. The dopant solution is produced by dissolving 100 mg of **OA** in 10 mL of dichloroethane. The SWCNT films are then soaked in the dopant solution for 1 h at 70 °C. The film is then rinsed with acetone to remove excess dopant molecules.

Measurements and Imaging. The sheet resistance of SWCNT films is measured with a standard four-point probe system

---

(20) Fuhrer, M. S.; Nygård, J.; Shih, L.; Forero, M.; Yoon, Y. G.; Mazzoni, M. S. C.; Choi, H. J.; Ihm, J.; Louie, S. G.; Zettl, A.; McEuen, P. L. *Science* **2000**, *288*, 494.
(21) Nirmalraj, P. N.; Lyons, P. E.; De, S.; Coleman, J. N.; Boland, J. J. *Nano Lett.* **2009**, *9*, 3890.
(22) Parekh, B. B.; Fanchini, G.; Eda, G.; Chhowalla, M. *Appl. Phys. Lett.* **2007**, *90*, 121913.
(23) Zhou, W.; Vavro, J.; Nemes, N. M.; Fischer, J. E.; Borondics, F.; Kamarás, K.; Tanner, D. B. *Phys. Rev. B* **2005**, *71*, 205423.
(24) Skakalova, V.; Kaiser, A. B.; Dettlaff-Weglikowska, U.; Hrncarikova, K.; Roth, S. *J. Phys. Chem. B* **2005**, *109*, 7174.
(25) Dettlaff-Weglikowska, U.; Skakalova, V.; Graupner, R.; Jhang, S. H.; Kim, B. H.; Lee, H. J.; Ley, L.; Park, Y. W.; Berber, S.; Tomanek, D.; Roth, S. *J. Am. Chem. Soc.* **2005**, *127*, 5125.
(26) Jackson, R.; Domercq, B.; Jain, R.; Kippelen, B.; Graham, S. *Adv. Funct. Mater.* **2008**, *18*, 2548.
(27) Arnold, M. S.; Green, A. A.; Hulvat, J. F.; Stupp, S. I.; Hersam, M. C. *Nat. Nanotechnol.* **2006**, *1*, 60.

Scheme 1. Reaction of OA with a SWCNT

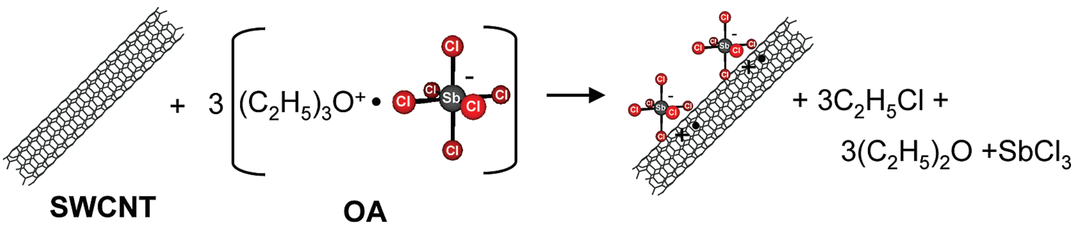

(Signaton). UV−vis-NIR spectra (λ = 400 nm to 2000 nm) of SWCNT films deposited over glass substrates are obtained with a spectrometer (Perkin-Elmer Lambda 950) using a blank glass substrate as a reference. Scanning electron microscope (SEM) images are taken at 1 kV beam voltage. Atomic force microscopy (AFM) is performed through noncontact mode in a Vicco AFM. Transmission electron microscope (TEM) images are taken at 120 kV (Philips TEM).

Results and Discussion

Figure 1a is an optical microscope image of a semitransparent film on a quartz disk. The atomic force microscope (AFM) image, shown in Figure 1b, reveals a penetrating, interlocking network of SWCNT bundles with diameters ranging from 10−20 nm. The AFM and TEM (Figure 1c) images reveal a film that is free of impurities and surfactant, a result of both the step-gradient purification step and an extensive cleaning procedure. The cleanliness of the SWCNTs films is a critical parameter affecting both the effectiveness of the doping and the stability of the resultant doped films. Figure 1d is a TEM image of a SWCNT film after doping with **OA**. The films are doped by dipping the film in a dilute solution of **OA**. The image reveals that the dopant accumulates on the side walls of the SWCNTs and at tube−tube junctions.

Chemical doping is achieved via the formation of a charge-transfer complex between the SWCNT and triethyloxonium hexachloroantimonate (**OA**) as illustrated in Scheme 1. The reaction involves transferring an electron from the SWCNT to produce the charge-transfer complex. Compound **OA** is a single-electron oxidant known to form a charge-transfer complex with aromatic compounds, including SWCNTs.[28,29] The $SWCNT^+$ and $SbCl_6^-$ ion form a stable charge-transfer complex, while C_2H_5Cl and $(C_2H_5)_2O$ are volatile byproducts. The reaction increases the hole density in the films, resulting in p-type doping. Since the metal salt is nonvolatile, the complex and thus the film resistance should be stable over time.

Figure 2a shows UV−vis-NIR absorption spectra for both undoped (black) and **OA** doped (red) SWCNT films. The undoped films were vacuum annealed prior to the measurement to ensure the removal of unintentional ambient dopants. The spectra reveal three main sets of absorptions bands that are attributed to the 1-D band structure of SWCNTs. The S11 absorption peak corresponds to the first set of Van Hove singularities above and below the band gap in semiconducting SWCNTs. Similarly, S22 and M11 peaks correspond to the second set of Van Hove singularities in semiconducting SWCNTs and the first set in metallic SWCNTs, respectively. When **OA** reacts with the SWCNT, an electron is transferred from the SWCNTs. The depletion of electrons from the valence band leads to an attenuation of the absorption peaks and is strong evidence of charge-transfer doping.[23] This is observed in the red trace of Figure 2a. The spectra show complete and near-complete attenuation of the S11 and S22 peaks of the semiconducting SWCNTs, respectively. As the electrons are depleted from the film, the hole carrier density increases, leading to effective p-type doping.

A plot of transmittance (%T at 550 nm) versus sheet resistance for undoped (purple), as-prepared (black), and **OA** doped (red) films is shown in Figure 2b. As expected, the resistance decreases with decreasing transparency and increasing film thickness. The sheet resistance was measured via standard four-point probe measurements. An important figure of merit for any transparent conductor is given by the following equation.[3]

$$\sigma/\alpha = -\{R_s \ln(T+R)\}^{-1} \qquad (1)$$

where σ and α are the dc conductivity and optical absorption coefficient, respectively. R_S is the nanotube film sheet resistance, T is the film transparency, and R is the film reflectance. The as-prepared films have a σ/α of 0.055 as shown in the black curve of Figure 2b. It is important to note that the as-prepared films are unintentionally doped via exposure to ambient dopants in the air. A series of films were fabricated, vacuum annealed, and then immediately measured. These films are labeled undoped (purple trace) and have a σ/α of 0.032. After **OA** doping, the ratio increases to a value of 0.13. This represents a factor of ~2.4 and ~4 increase relative to the as-prepared and vacuum annealed films, respectively. This increase in σ/α is comparable to increases observed with concentrated acid baths that are typically employed (i.e., HNO_3 and $SOCl_2$).[18,25] These ratios correspond to films (with a %T of 75% at 550 nm) with an R_s of 246 $\Omega/\square$ for the undoped film, 152 $\Omega/\square$ for the as-prepared film, and 63 $\Omega/\square$ for the **OA** doped film. Another common figure of merit is the ratio σ_{dc}/σ_{op}, where σ_{dc} is the dc conductivity, and σ_{op} is the optical conductivity. A full description of both fitting methods and our rationale for choosing to display the data using eq 1 is included in Supporting Information.

---

(28) Rathore, R.; Kumar, A. S.; Lindeman, S. V.; Kochi, J. K. *J. Org. Chem.* **1998**, *63*, 5847.

(29) Chen, J.; Klinke, C.; Afzali, A.; Avouris, P. *Appl. Phys. Lett.* **2005**, *86*, 123108.

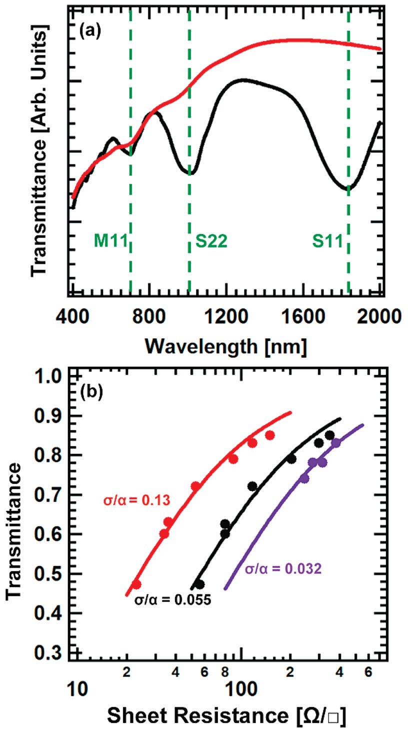

Figure 2. (a) UV−vis-NIR spectra of undoped (black) and doped (red) carbon nanotube films illustrating the attenuation of the optical transitions due to chemical doping with OA. (b) Plot of transmittance versus sheet resistance of undoped (purple), as-prepared (black), and OA doped (red) SWCNT films. The solid lines are a fit to eq 1.

As **OA** is a nonvolatile metal salt, the stability of **OA**-doped films was studied and compared to films doped with HNO_3. Figure 3a is a UV−vis-NIR spectrum of a film doped with nitric acid taken at various times from immediately after doping to 98 h after doping. The initial spectra shows very effective doping, with both the S22 and S11 absorption region completely attenuated. As the HNO_3 desorbs, the S22 transitions begin to regain their oscillator strength. The S22 peaks rapidly increase in intensity and after 23 h, and the S11 transitions start to gain strength and continually increase through 98 h after doping. The spectrum taken at 98 h reveals an S22 region that has regained virtually all of the original strength and a small peak at the S11 region. These changes indicate a drastic reduction in the hole carrier density and a dedoping of the film. In contrast, the **OA** doped film is remarkably stable. The S22 region displays very little change over the course of the study. There is an initial, small increase in the S22 peaks that saturates over time. The S11 region shows virtually no change after 98 h of air exposure. The data implies that the increased hole-carrier density in the **OA** doped film is stable over time, in stark contrast to the unstable HNO_3 films.

Figure 4a is a plot of the transmittance at the S22 peak versus time for both **OA** and HNO_3 doped films. The data was extracted from the absorption spectra in Figure 3a and b. A decrease in the transmittance represents an increase in the S22 peak height and, therefore, dedoping of the film. Although only relative differences are considered here, the two films have comparable transparencies (% T of 56.3 and 60.7 at 550 nm for HNO_3 and **OA** doped films, respectively). The **OA** doped film shows a slight drop during the first few hours, followed by saturation in the peak height over time. In contrast, the HNO_3 doped film shows a large drop in the transmittance, followed by saturation after 24 h of exposure. This follows what was observed in Figure 3a and b. The correlation between this optical data and the electrical data in Figure 4b is striking. Figure 4b is a plot of σ/α versus time for both **OA** and HNO_3 doped films. Since the transparency at 550 nm does not change with time, the change in σ/α is exclusively due to changes in the electrical conductivity. The change in σ/α over time for the **OA** doped film is virtually identical to the red curve in Figure 4a, showing a slight, initial drop followed by saturation. The optical data proves to be an excellent predictor of the electrical performance of the film. The change in σ/α for the HNO_3 doped film also closely follows the blue curve in Figure 4a, but diverges at 24 h postdoping. While the change in the S22 peak saturates, the conductivity continues to decrease in the HNO_3 doped films. The S22 peak regains nearly all of the original oscillator strength, and therefore, the blue curve in Figure 4a saturates. Although the S22 peak has saturated, after 24 h the S11 peak begins to increase over time as the film continues to dedope (illustrated in Figure 3a). This continual dedoping of the film results in σ/α decreasing for the duration of the study. The dotted green lines indicate when the **OA** doped films begin to out perform the HNO_3 films. After 98 h postdoping, σ/α of the HNO_3 doped film decreases to a value of 0.05 from 0.14, decreasing by a factor of 3. As shown in Figure 2b, this final value is comparable to those of as-prepared films. In the case of HNO_3 doping, the doping and associated decrease in sheet resistance is gone after a few days. In stark contrast, σ/α of the **OA** doped films decreases

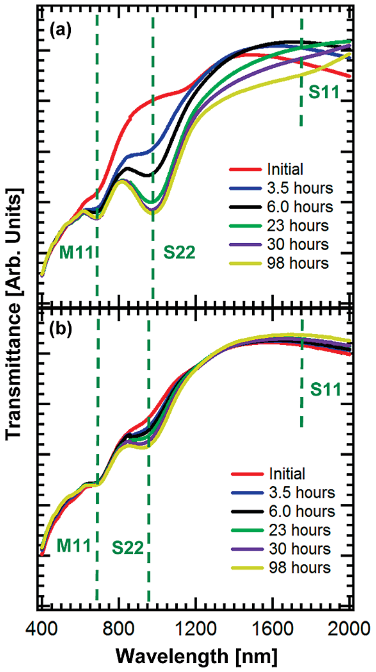

Figure 3. UV−vis-NIR spectra as a function of time of SWCNT films after doping with (a) nitric acid and (b) **OA**. The **OA** doped films are significantly more stable compared to the nitric acid doped films.

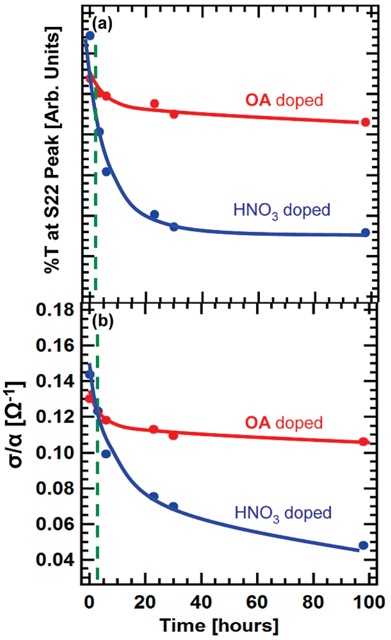

Figure 4. (a) Plot of %T at the S22 peak versus time for SWCNT films doped with **OA** (red) and nitric acid (blue). (b) Plot of σ/α versus time for SWCNT films doped with **OA** (red) and nitric acid (blue). The dotted green lines indicate at what point the OA doped films begin to outperform the nitric acid doped films.

slightly, by ~15%, reaching a value of ~0.11. This value is still a factor of ~2 larger than that of as-prepared films and a factor of 3 larger than that of the undoped films.

Conclusions

In conclusion, we have demonstrated that SWCNT films can be effectively doped with a metal salt via electron transfer from the carbon nanotube. This was confirmed via UV−vis-NIR spectra and electrical measurements of films doped with **OA**. The **OA** doped films are stable over time, as compared to films doped with nitric acid. The films doped with nitric acid reach their initial, predoping values after several days, while the **OA** doped films maintain their increased conductivity. The optical data of the film correlated strongly to the electrical data and proved to be a good predictor of how the films behave over time. This work presents a new category of chemical dopants for the fabrication of stable, transparent, and conductive SWCNT films.

Acknowledgment. We thank Ageeth Bol for TEM images and S. Guha and J. B. Hannon for helpful discussions.

Supporting Information Available: Transmission electron microscope (TEM) images of carbon nanotube films before and after acid/water cleaning (Figures S1a, S1b); discussion regarding another widely used figure of merit (σ_{dc}/σ_{op}) for transparent conductors; transparency vs sheet resistance graphs (Figure S2) with air doped films, dedoped films, nitric acid doped, and antimony doped films, curve fitted with the discussed figure of merit. This material is available free of charge via the Internet at http://pubs.acs.org.